Dynamic simulation and configuration dependant modal identification of a portable flexible-link and flexible-joint robot

Grzegorz Swiatek[1], Zhaoheng Liu[1] and Bruce Hazel[2]

[1]Department of Mechanical Engineering, École de technologie supérieure (ÉTS), Université du Québec
Montreal, Quebec, Canada H3C 1K3
[2]Institut de recherche d'Hydro-Québec (IREQ)
Varennes, Quebec, Canada J3X 1S1

ABSTRACT

A 6 DOF robot dedicated to repair hydroelectric equipments is analyzed in this study. A generic approach is proposed to conduct dynamic simulation using MD Adams software and to identify modal information at the system level for any given configuration of the robot. Four out of six links of the robotic system are modeled by flexible bodies, pre-processed by finite element method. The meshed flexible bodies derived from the CAD geometry, containing modal information are then integrated in the dynamic model. The flexibility of 6 joints is also incorporated in the model using their joint stiffness obtained from actuators' internal components properties. The vibrational behaviour of the robotic system will be presented for a set of pre-programmed trajectories. Moreover, the vibration modes resulting from flexible links and flexible joints can be determined for any configuration of the robot in the workspace. This model is validated by comparing 3D coordinates of the robot end effector measured from static experiments and from the simulation. This simulation model will be a very useful tool for further investigation of chatter vibration in robotic grinding for surface rectification.

RÉSUMÉ

Un robot à 6 degrés de liberté dédié à la réparation d'équipements hydroélectriques est étudié dans ce document. Une approche générique est utilisée afin de réaliser une simulation dynamique en utilisant le logiciel MD Adams afin de récupérer les informations modales du système pour n'importe quelle configuration donnée du robot. Quatre des six membrures du système robotisé sont modélisées avec des corps flexibles qui sont préalablement traitées dans un logiciel par la méthode des éléments finis. Les corps maillés flexibles provenant du modèle CAD et qui contiennent les informations modales sont ensuite incorporés dans le modèle dynamique. La flexibilité des 6 joints est également incorporée dans le modèle en utilisant les rigidités des joints obtenues expérimentalement. Le comportement vibratoire du système robotique sera présenté pour une série de trajectoires préprogrammées. De plus, les modes de vibration provenant des joints et membrures flexibles pourront être déterminés pour n'importe quelle configuration dans l'espace du robot. Le modèle sera validé en comparant les résultats de la simulation avec les coordonnées 3D du 'end-effecteur' du robot mesurées par essais expérimentaux. Ce modèle de simulation sera un outil très utile pour l'étude du meulage robotisé de grande précision par les robots portables flexibles.

1. INTRODUCTION

In the context of hydroelectric industry equipments, cavitation and cracking, observed on turbine wheels, are phenomena that affect the overall efficiency and optimal output of turbine-generators. In order to overcome these problems, the Research Institute of Hydro-Quebec developed a robot system that performs automatically multiple maintenance and repair processes of turbine runners. Since the grinding, hammer peening, welding, plasma-gouging and high-precision grinding processes on hydroelectric equipments have been automated, they have become more efficient, and operational costs have been reduced. Being compact and lightweight, the 6 degrees-of-freedom robot is designed to be installed on a track quickly to perform specific repairs and maintenance operations [1]. This robot, entitled "SCOMPI" (Figure 1), can reach areas and sections that are inaccessible to humans. Moreover, being compact and portable, SCOMPI is less rigid than other industrial robots. In this project, a virtual model of the most recent version of SCOMPI (third generation) is developed in an attempt to understand and analyze the vibrational behaviour of the system, and to propose methods to reduce the negative effects of vibration. The model and simulation of the robot have been created, bearing in mind the flexibility of its joints and links. This modeling method enables us to identify modal information for any given configuration and to determine end effector positions during robot operations more accurately.

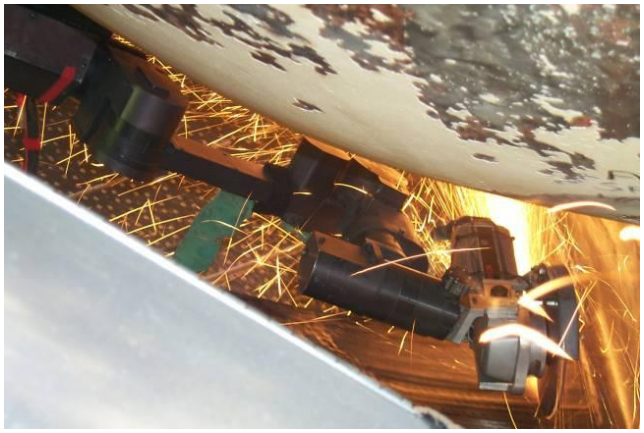

Figure 1 - SCOMPI robot developed by Research Institute of Hydro-Quebec

Virtual prototyping and dynamic simulation is becoming more popular as personal computers and workstations become more powerful, and as computer-aided design programs become more than simple drawing tools. Different CAD programs now include a module to perform dynamic simulations in order to analyze the dynamic characteristics of a system under various loads and conditions. Such tools enable the user to create a variety of dynamic joints between components, to add motions, implement forces, specify contacts, include friction forces, consider gravity and take the physical properties of the components into account. Furthermore, the user can extract result parameters such as speed, the position, the force, the torque, the acceleration or the force of reaction of any given component from the model at any moment during the simulation and then present it in the form of numerical analysis, a graphic chart or a

trace in the model environment. Nowadays, computer-aided engineering programs offer tools to analyze multi-body dynamic simulations, thermal and fluid flow analysis, structural mechanics, multi-physics, optimization, control systems, linear and nonlinear finite element analysis and more.

On the side of fundamental and theoretical formulation and study of the flexible multiple body mechanical systems, numerous research works have been published over the last two decades. Floating frame of reference formulation and finite-element formulation are widely used to establish deformable body dynamic equations [2]. Computational methods have been developed for the dynamic analysis of multi-deformable body systems [2 - 5]. In the case of this study, the existing CAD model is available in the CATIA V5R18 program format. The finite element method capabilities of the ANSYS V12.0 program were used to generate the meshed flexible bodies, while MSC MD Adams was used for the simulation. MSC Software provides a set of programs such as MD Adams, Nastran, Patran intended for various multidisciplinary applications related to engineering. In this research work, Adams/View was used as a base for the simulations and Adams/Flex along with Adams/Vibration were used to integrate the flexible bodies, analyze the modes and frequencies and to inspect other vibrational characteristics. For the robots with flexible link and flexible joints such as SCOMPI, a simple dynamic simulation of the model with translational and rotational joints is not sufficient because the effects of deflection and deformation of links and joints are neglected, resulting in a rigid model that doesn't behave in a realistic manner. Advantages of using Adams/Flex include capturing inertial and compliance properties during simulations, predicting loads with greater accuracy by allowing Adams to account for flexibility during simulations, and obtaining accurate information about the deformation of a component.

2. MODELCONSTRUCTION IN MD ADAMS

The very first step of the modeling process is to create a rigid dynamic simulation of the model within Adams/View. The purpose of this simulation is to ensure that the model is functional in the Adams environment and therefore that subsequent actions can be performed to implement flexibility to the joints and links. Moreover, the rigid model and simulation will be useful to compare results with the flexible model later. Using the available CAD model of SCOMPI in CATIA V5 (Figure 2), each robot link is simplified and exported using a neutral format, in this case, the STEP format. Typical simplifications to the model include the suppression of holes, fillets and unnecessary details. These modifications are recommended to facilitate changing it into a neutral format, and also because the model will be meshed later on with the finite element method. Once bodies are simplified, the model is assembled in the Adams environment using translational joints, revolute joints and imposed motions (J1: translational joint, J2-J6: revolute joints). Markers are added to each joint for future use of virtual measurement sensors and to ease the insertion of the flexible components.

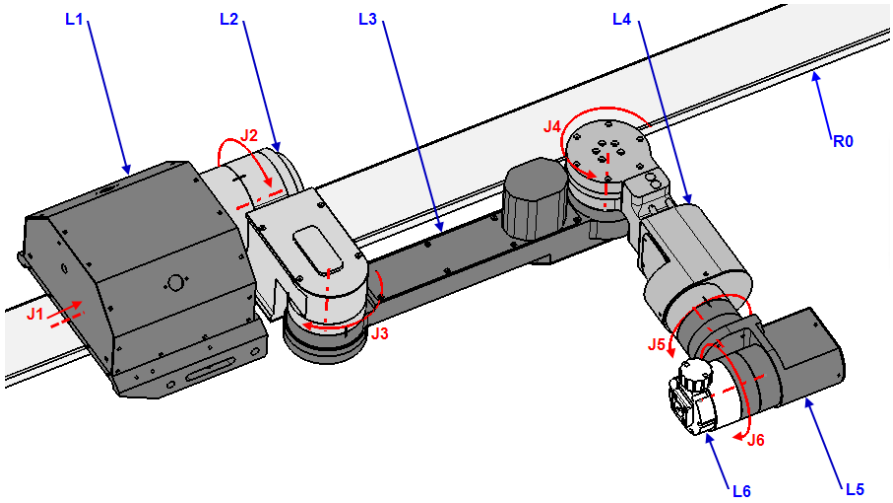

Figure 2- CAD Model of the robot – Links and Joints

Once the rigid simulation is fully functional, flexible bodies are created. Different finite element method (FEM) programs can be used to generate a file that contains the flexible body characteristics, ANSYS 12.0 has been chosen for this particular operation. When creating a flexible part, the output file generated is named a modal neutral file (MNF) and contains information such as geometry (location of nodes and node connectivity), nodal mass and inertia, mode shapes, generalized mass and stiffness for modal shapes.

For each MNF file (links L2, L3, L4 and L5), the same steps are followed; the simplified part from the STEP format is imported into ANSYS, material properties are assigned (density, Young's modulus, Poisson's ratio), elements are assigned (SOLID45, BEAM4) and their real constants, the volume is meshed, two interface points are modeled (used as connection nodes in the Adams model), support beams between the interface nodes and the volume are added, units are chosen (m, s, kg, N), the number of modes to be exported are determined (20 modes) and finally, solved and exported to the MNF format. Each link is composed of about 3 000 to 5 000 nodes per volume, 2 interface nodes and a total of about 20 support beams (Figure 3).

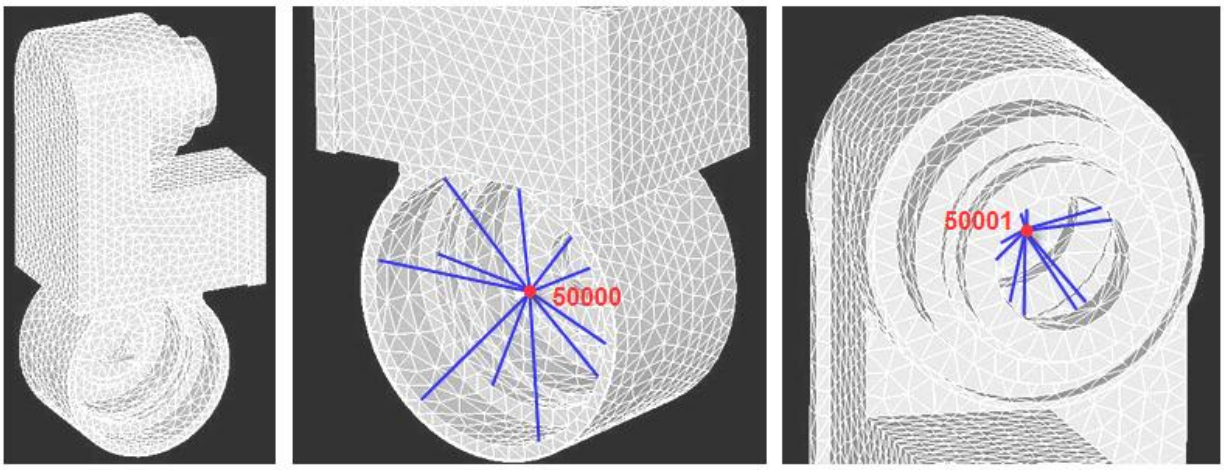

Figure 3 – Mesh, support beams and interface points for link L2

An interface point is a node that will have an applied joint or force in the Adams program; forces can only be applied to interface points. Those points will be used to position the component precisely within the Adams model; in this case, interface points are connected to the markers created in the rigid model. The role of the support beams is to distribute the force over an area instead of on a single node. Those beams have a high stiffness and a small mass. The final important procedure is the adjustment of the density of each link. Since many internal components are not represented in the meshed model due to their complexity (motor, encoder, harmonic drive etc), the density of each link in the simulation is adjusted to match the mass of the real component in real-life. This means that the mass is valid, but the fact that it is equally distributed in the volume makes slight changes in the center of gravity position and the values of inertia of the model.

Once each MNF is generated, the flexible-link model is created by swapping the rigid bodies by flexible bodies one-by-one (Figure 4). Once the L2 to L5 links have been replaced by flexible components, flexible joints are added to the model. Special attention and care is needed for this operation, bearing in mind that the joints of the robot are affected by imposed motions in the Adams model. An imposed motion on a joint cancels the effect of a spring, whether it is a torsion spring or a translational spring. For this reason, a dummy part is added to each joint (J1 to J6) that connects a spring to the next link, while the rotation between the previous link and the dummy part is motion controlled. At the same time, joint stiffness assigned to each spring is obtained from actuator's internal reducer and motor properties and the value is constant.

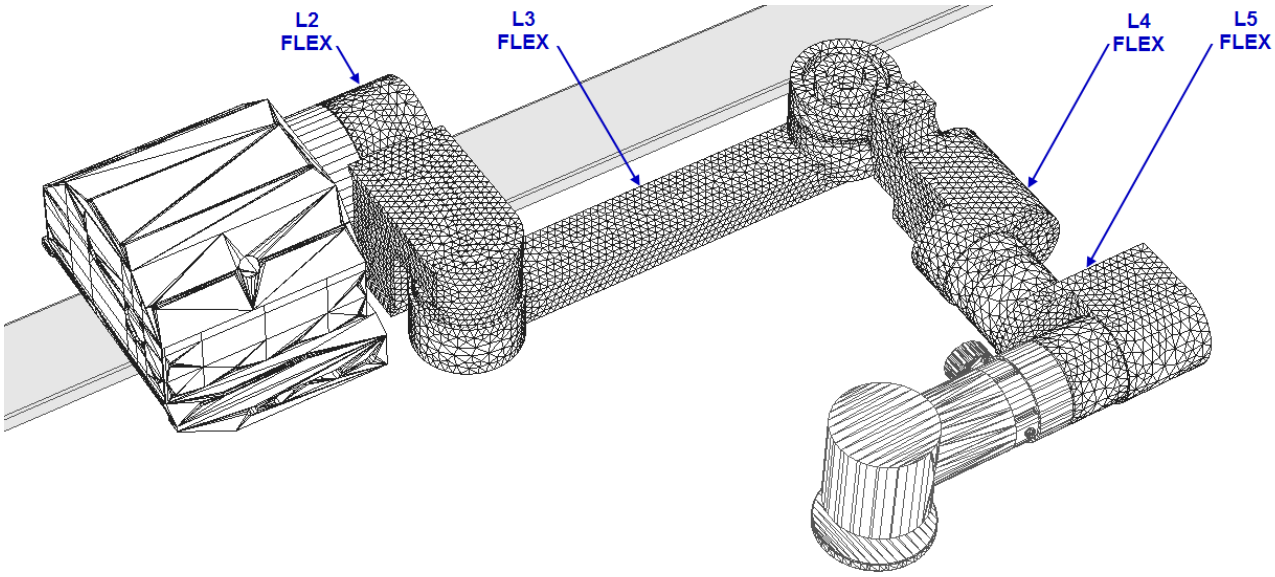

Figure 4 – Meshed flexible-link model of the robot in Adams/View

3. SIMULATION RESULTS

A rigid simulation is created using rigid parts, MNF flexible bodies are generated and flexible joints are added to the model, which provided an opportunity to use and compare 4 different models within Adams:

I. Rigid model
II. Flexible-link model
III. Flexible-joint model
IV. Flexible-link and Flexible-joint model

3.1 Dynamic Simulation with imposed motion

To compare the 4 models, motion is imposed to each joint to produce a movement of the robot – results such as the position of the end effector (the point at the end of the last link of the robot arm) can be inspected. The motions are applied directly to the joints, allowing control on translational displacement (J1) and rotational displacement (J2, J3, J4, J5 and J6) to produce a 4.5 seconds sequence. The motions are represented in the form of graphs, and the start position and end position is illustrated (Figure 5). In Figure 5, the values for translational and rotational displacements are given using a function of time (STEP5 function). Once the sequence is

complete for all the models (I, II III and IV), results can be saved and the Adams/PostProcessor will be used in the plotting and animation environment, and to review and analyze the results. The advantage of presenting the results in this environment is the possibility to overlay various simulations and results.

Figure 6 is a graph of the X position of the end effector of the robot for a 4.5 seconds simulation. All four models are presented on this multi-layer graph for the total time. Figure 6 shows that the flexible-link (II) curve is right over the rigid (I) model curve, while the flexible-joint (III) or the flexible-joint and flexible-link (IV) curves are at a much higher distance from the rigid curve. Joint-flexibility needs to be quantified.

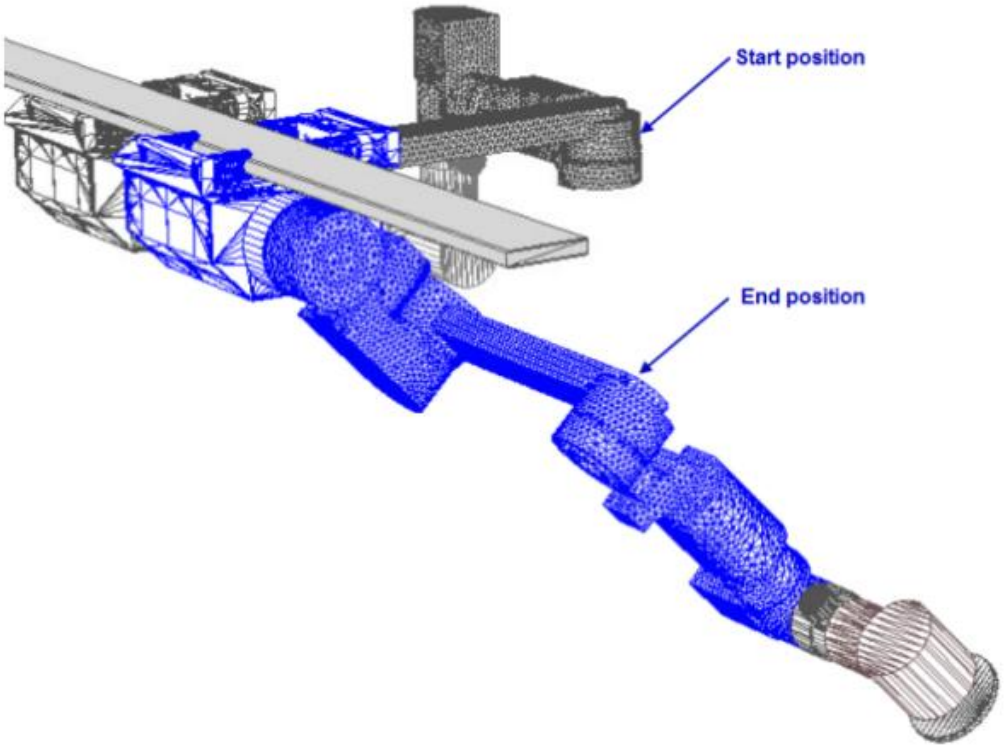

Joint	Joint type	Displacement versus time
J1	translational	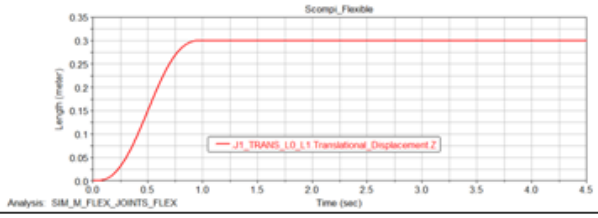
J2	revolute	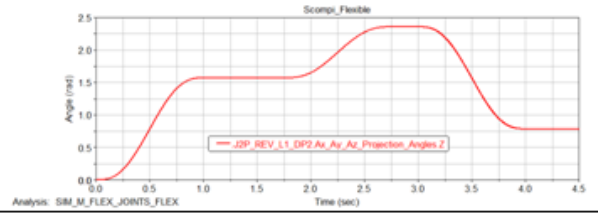
J3	revolute	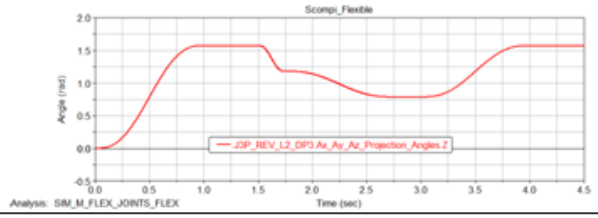
J4	revolute	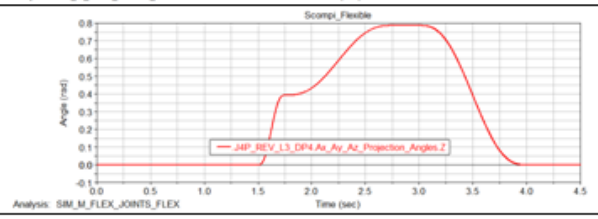
J5	revolute	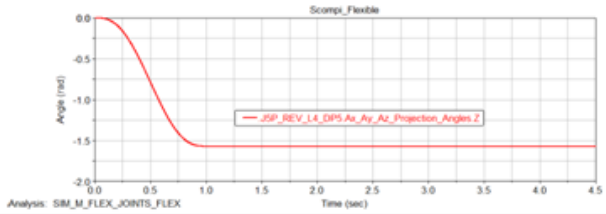
J6	revolute	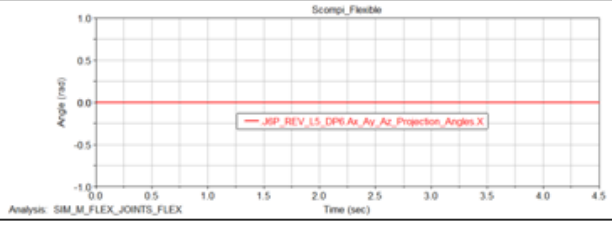

Figure 5 - Imposed motion for each joint, start and end positions

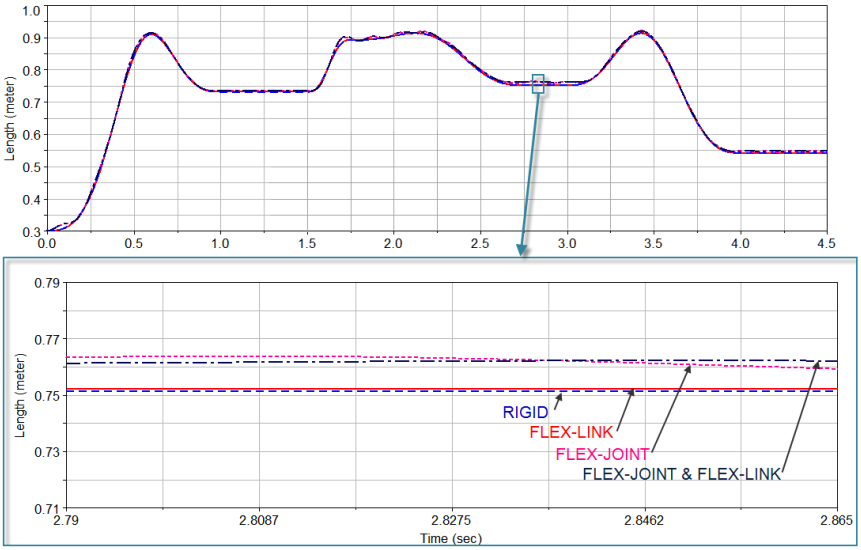

Figure 6 - Comparison of the X position of the end-effector for 4 models (with zoom on a small section)

3.2 Determination of static equilibrium positions

The previous graphs are results of a dynamic simulation performed in a defined time. Another way to analyze the model is by finding static equilibrium positions. To achieve this, the solver of MD Adams iteratively repositions every part in an attempt to balance all the forces [6]. The flexibility of joints and links are considered. Four different configurations are evaluated (A, B, C and D) and for each model (I, II, III and IV), the static equilibrium is performed. Using a measurement sensor, the distance between the absolute origin of the assembly (inside part J1, close to the track) and the end effector is recorded.

In Table 1, the last column shows the percentage of deformation compared to the rigid simulation. Based on those values, the flexibility of joints contributes to about 92% of the total deformation of the system, while the flexibility of links contributes to approximately 8%. One important step for future studies will be to take into account the nonlinear behaviour of the harmonic reducers in the model, and to monitor variable joint-stiffness values depending on the load applied. The robot's track torsion and robot attachment to the track should also be considered.

Table 1 – Vertical coordinate of the end effector for 4 static equilibrium positions (A, B, C and D) for 4 models (I, II, III and IV)

Configuration A	Configuration B	Configuration C	Configuration D
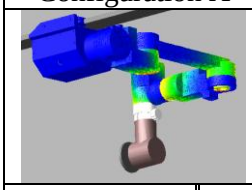	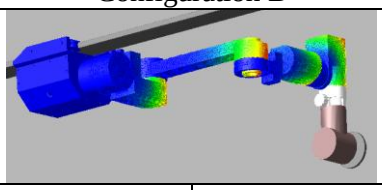		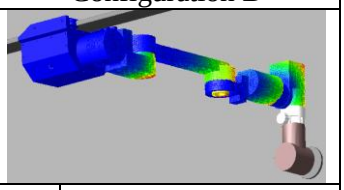

Configuration	Joint displacements (m or rad)	X position (m) for the 4 models (static equilibrium)		Percentage of deformation compared to the rigid simulation (%)
A	J1=0 J2=0 J3=0 J4=0 J5=0 J6=0	Rigid (I) Flex-link (II) Flex-joint (III) Flex-link and Flex-joint(IV)	0.3007 0.3014 0.3093 0.3100	0.0000 7.5269 92.4731 100.0000
B	J1=0 J2=0 J3= -pi/2 J4=0 J5=0 J6=0	Rigid (I) Flex-link (II) Flex-joint (III) Flex-link and Flex-joint (IV)	0.3007 0.3014 0.3074 0.3081	0.0000 9.4595 90.5405 100.0000
C	J1=0 J2= -pi/2 J3= -pi/2 J4=0 J5=0 J6=0	Rigid (I) Flex-link (II) Flex-joint (III) Flex-link and Flex-joint (IV)	0.7309 0.7312 0.7334 0.7336	0.0000 11.1111 92.5926 100.0000
D	J1=0 J2= 0 J3= 0 J4=-pi/2 J5=0 J6=0	Rigid (I) Flex-link (II) Flex-joint (III) Flex-link and Flex-joint (IV)	0.3007 0.3021 0.3211 0.3224	0.0000 6.4516 94.0092 100.0000

3.3 Joints deformation

On each translational or revolute joint (J1 to J5), a measurement sensor is added in order to capture information about the real deformation of the joint. Similar sensors are added to the dummy part of each joint to record the values of the theoretical imposed motions. Finally, values can be examined side-by-side for any given configuration to note, independently, the deformation of each joint. Figure 7 shows the output data of the sensors of each joint and the

real deformations; in this case, no movement is imposed, and only the static equilibrium position is found after a period of damped vibrations.

JOINT	Joint deformation (m) (over 4.5 seconds)
J1	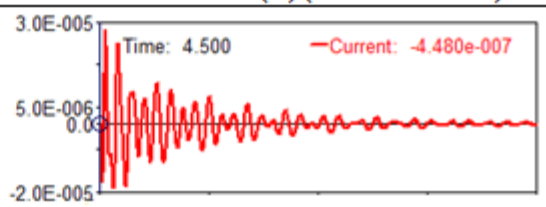
J2	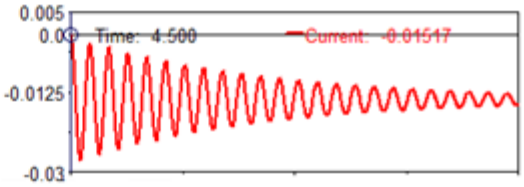
J3	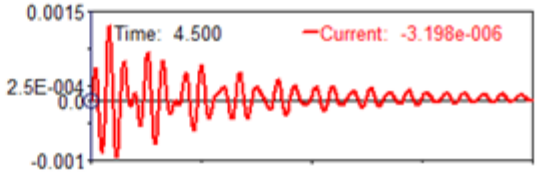
J4	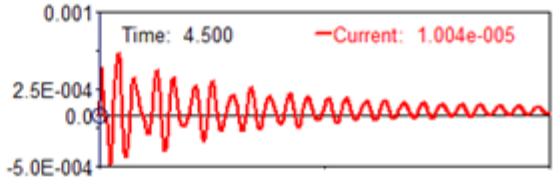
J5	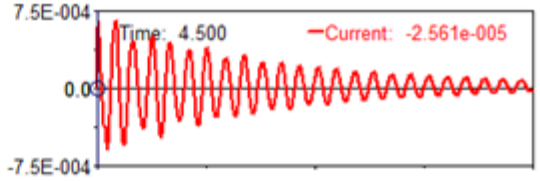

Figure 7 - Joints deformations at the Configuration A

Table 2 – Angular displacements of joints at the Configuration A measured by sensors

Model	Displ. J1 (mm)	Angle J2 (deg)	Angle J3 (deg)	Angle J4 (deg)	Angle J5 (deg)
Rigid (I)	0.00000	0.00000	0.00000	0.00000	0.00000
Flex-joint (III)	0.00000	0.81131	0.00247	0.00217	0.00100
Flex-link and Flex-joint (IV)	0.00000	0.81131	0.00250	0.00230	0.00107

The results listed in Table 2 show that joint and link flexibility has an influence on the position of the robot and the angular displacements of the joints.

4. VIBRATION AND MODAL ANALYSIS

The model built in Adams that contains flexible links and joints allows extraction of the vibration modes for the robot in any configuration. This means that the simulation can be stopped at any moment, the static equilibrium position found, and natural frequencies, modes and damping ratios can be obtained. The results of the first 8 modes for configurations A and B are listed in Table 3.

Table 3 - Modal analysis for configurations A and B

MODE NUMBER (Configuration A)	UNDAMPED NATURAL FREQUENCY (Hz)	DAMPING RATIO
1	5.284940E+000	1.557673E-002
2	7.644467E+000	2.145779E-002
3	1.735447E+001	4.982392E-002
4	3.173958E+001	9.441490E-002
5	3.542305E+001	9.496859E-002
6	4.529875E+001	1.883755E-002
7	1.069312E+002	3.312767E-001
8	1.827252E+002	2.457449E-002

MODE NUMBER (Configuration B)	UNDAMPED NATURAL FREQUENCY (Hz)	DAMPING RATIO
1	6.706954E+000	1.889229E-002
2	7.726440E+000	2.181063E-002
3	1.779301E+001	5.226387E-002
4	2.805010E+001	8.381574E-002
5	3.481670E+001	9.632134E-002
6	6.763493E+001	1.403289E-002
7	1.070813E+002	3.314308E-001
8	1.097215E+002	4.096556E-002

Modes can also be viewed and animated for any configuration during simulation, enabling us to visualize the participation to the modal deformation for each degree of freedom of the joints and the links.

Another analysis is performed using an unbalanced rotating mass positioned on the grinding wheel. The point mass positioned on the rotating wheel causes imbalance and vibrations. The mass used weighs 4.0E-003 kg; it is placed at 0.01m from the rotation axis. This corresponds to a grinding wheel of 1.9kg offset of 0.5mm, which is typical. The grinding wheel is rotating at 200π rad/sec (6000 RPM). The flexible-joint model is used in this simulation. Figure 8 shows the

simulation results (vertical displacement of the end effector) with and without an unbalanced rotating mass on the grinding wheel. The effect of the unbalanced force can be seen from the trajectories. It is interesting to notice that the oscillation of the end effector caused by an unbalanced rotating mass appears with the first natural frequency of the robotic system.

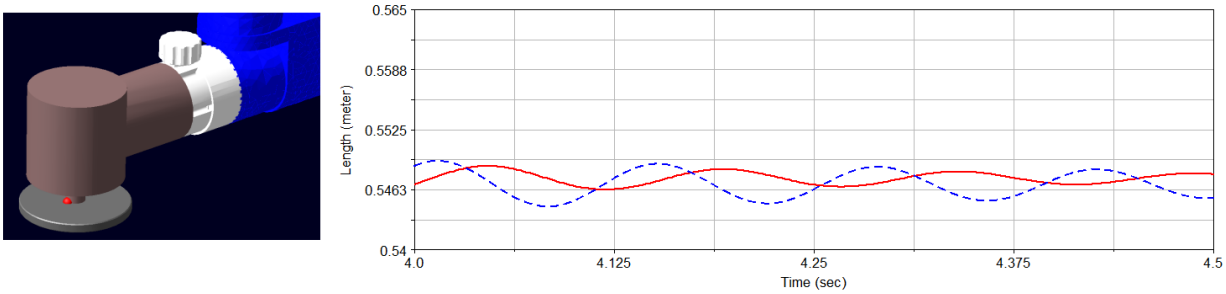

Figure 8 - Effect of an unbalanced rotating mass on the grinding wheel (dashed curve)

5. MODEL VALIDATION

This model is validated by comparing 3D coordinates of the robot's end effector measured from both experiments and simulation. The experiments conducted by the Institute of Research of Hydro-Quebec consisted of suspending masses at the end of the robot (0, 5, 10, 15 and 20 pounds) for 20 different positions and the measurement of the angular and translational displacements of the end effector were recorded. The same setup is implemented in the Adams model and displacements are read from the virtual sensors for every mass added. This is the first validation between the 3D model and the robot – based on those results; it will then be possible to refine the model by taking into account various other factors such as the non-linear behaviour of the harmonic drive reducers, the bearings lateral deflections, the track and the distribution of the link's weight.

An Optotrak system, from Northen Digital, is used to measure manipulator displacement as different load masses are attached to the end effector. 13 markers are mounted on a half sphere as shown on Fig. 9. At least 6 to 7 markers are always visible from the Optotrak depending on the orientation of the half sphere. Once the positions of all visible markers have been acquired, a similarity transform [7] is used to optimize the position/orientation of the half sphere from the theoretical locations of the markers on the half sphere. The first ten 10 were performed on a horizontal track (gravity normal to the track) and the last ten on a vertical track (gravity aligned to the track) to make sure that displacement are generated on all joints.

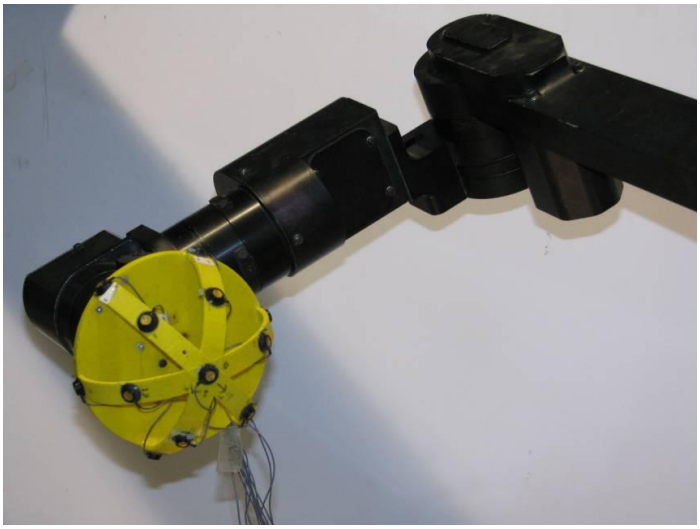

Figure 9 Optotrak markers installed on a half sphere mounted to the robot

Small displacements in Cartesian space $\delta\chi$ are related to joint displacements $\delta\theta$ through the manipulator's Jacobian J as stated in (1)

$$\delta\chi = J\delta\theta \tag{1}$$

In the force domain, the joint torques τ are related to the Cartesian force-moment vector F such as

$$\tau = J^T F \tag{2}$$

The compliance of each joint is modeled according to the following linear equation that relates the joint displacements $\delta\theta$ to joint torques τ

$$\delta\theta = c\tau \tag{3}$$

$$c = \begin{bmatrix} c_1 & & & & & \\ & c_2 & & & & \\ & & c_3 & & & \\ & & & c_4 & & \\ & & & & c_5 & \\ & & & & & c_6 \end{bmatrix}$$

where **c** is the joint compliance matrix and c_1 to c_6 are the compliances of joint 1 to 6. In Cartesian space, the displacements $\delta\chi$ resulting from a force-moment vector F could be computed from the Cartesian compliance matrix C_W as given below

$$\delta\chi = C_W F \tag{4}$$

The compliance in Cartesian space can be related to the compliance in joint space as written below

$$C_W = JcJ^T \tag{5}$$

In order to estimate the joint compliance of the manipulator, a series of experiments were carried on where forces where applied to the manipulator's end effector while measuring the

resulting Cartesian displacements. The joint compliance is then estimated by minimizing the rms error between the N model and measured displacements as given below

$$e^2 = \frac{1}{N}\sum_{n=1}^{N}\left\| J_n c J_n^T F_n - \delta\chi_n \right\|^2 \tag{6}$$

This is accomplished by solving the following normal equation

$$Ac = b \tag{7}$$

$$A = \sum_{n=1}^{N}\left(J_n^T J_n^T F_n\right)^T J_n^T J_n^T F_n$$

$$b = \sum_{n=1}^{N}\delta\chi_n^T J_n^T J_n^T F_n$$

Table 4 presents the values of joint compliance obtained from the actuators internal components properties as compared to the values obtained by solving equation (7) with N=80 displacement measurements (20 robot position x 4 different weights).

Table 4 - Comparison of joint stiffness obtained from components properties and experimental measurements

		Joints					
		1	**2**	**3**	**4**	**5**	**6**
Components Stiffness							
motor stiffness	Nm/rad	276.5	85.0	85.0	85.0	47.3	47.3
motor reflected stiffness	kNm/rad	14.10	38.24	19.93	21.25	10.08	7.56
harmonic drive stiffness	kNm/rad	13.56	58.18	26.44	26.44	13.56	13.56
track torsional stiffness	kNm/rad		26.20				
Total joint stiffness	kNm/rad	*6.91*	12.27	11.36	11.78	5.78	4.85
	kN/m	1058.0					
Optimized stiffness	kNm/rad		6.75	11.15	12.72	4.78	3.00
	kN/m	776.4					

The theoretical joint compliance value of each actuator is obtained by adding the compliance of the harmonic drive reducer (as provided by the manufacturer) to the compliance of the motor reflected to the reducer. The motor compliance is obtained from the following approximation

$$c_M = \frac{2\pi}{3\tau_H}$$

where τ_H is the motor holding torque. The motor reflected stiffness is obtained by multiplying by the reducer ratio. The total joint stiffness obtained is well in accordance with the values optimized from the experimental data set except for joint #2 which was optimized to a much lower stiffness value. If the track torsional compliance is added to joint #2, which is parallel to the track and close to it, the difference becomes less important.

The residual error on the displacement after solving the system given in (7) is shown in Table 5. It is observed that this simple joint compliance model explains about 80% of the Cartesian displacements. The translation accuracy is better than the one in rotation.

Table 5 - Residual error after optimization of the experimental data set

		epx(mm)	epy(mm)	epz(mm)	erx(deg)	ery(deg)	erz(deg)
Displacement							
	RMS	1.791	1.348	2.817	0.281	0.189	0.113
	Max	5.089	4.6	10.569	0.830	0.517	0.334
Error							
	RMS	0.265	0.421	0.522	0.051	0.105	0.049
		14.8%	31.2%	18.5%	18.2%	55.8%	43.5%
	Max	0.928	1.767	1.815	0.160	0.446	0.147
		18.2%	38.4%	17.2%	19.3%	86.2%	43.9%

The positions evaluated during the experiments are reproduced within the Adams environment. For each position of the flexible-joint robot, the static equilibrium position is obtained for the 0, 5, 10, 15 and 20 pounds suspended masses. The position of the end effector is measured and the deformations are calculated and then compared to the experimental results. Table 6 shows values imposed to each joint for one experimental position, Figure 10 shows the position of the robot and Table 7 shows the values of deformations of both models including the percentage between the experimental and Adams model values.

Table 6 – Example position joints values for J1 to J6

Joints positions	
J1(m)	0.109759
J2(deg)	-2.8222
J3(deg)	49.6593
J4(deg)	35.0452
J5(deg)	-204.6954
J6(deg)	-6.4666

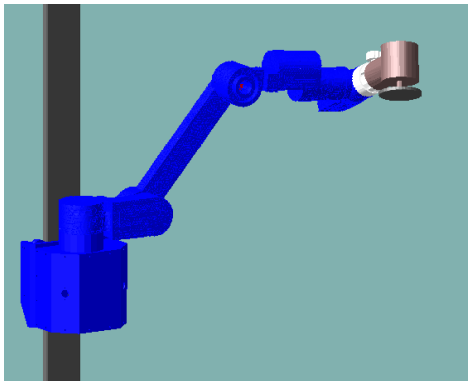

Figure 10 - Experimental position example within ADAMS

Table 7 - Comparison of experimental and model deformations for one experiment position

Force (pounds)	Experimental deform.(m)	Model deform. (m)	Difference(%)
0	0.000000	0.000000	0.000000
5	0.001083	0.001300	16.692308
10	0.002272	0.002700	15.851852
15	0.003427	0.004000	14.325000
20	0.004581	0.005300	13.566038

Table 7 displays values for one position, but the average of all the positions evaluated within the Adams model is also calculated. The average difference between the experimental model and the Adams model is 15.84 %, this value is calculated for all four suspended masses (5, 10, 15, 20 pounds).

6. CONCLUSION

Developed using a dynamic simulation program combined with a finite element approach, a 6 DOF flexible robot model was built to examine the effects of joint and link flexibility on its vibrational behaviour. Deformations under imposed motions were analysed, deflections of the robot during a static equilibrium position were observed, joints deformations were monitored and vibrational and modal analysis were performed on the robot. This model's validation is based on results from static experiments. The model will be refined by implementing non-linearity of the harmonic drives reducers, the lateral deflection of bearings and by distributing the mass more accurately on the links.

7. ACKNOWLEDGEMENTS

The authors would like to acknowledge the financial support provided by the National Sciences and Engineering Research Council of Canada (NSERC), the Institute of Research of Hydro-Quebec (IREQ) and the École de Technologie Supérieure (ETS). The first author conducted this research project through the NSERC Undergraduate Student Research Awards (USRA).

8. REFERENCES

[1] Fihey, J.-L., Hazel, B. Et Laroche, Y., 'The Scompi Technology', *Proceedings of the Int. Forum on Situ Robotic Repair of Hydraulic Turbines*, 11-12 Nov., 2000, Harbin, China.

[2] Shabana, A.A., '*Dynamics of Multibody Systems'*, Cambridge University Press, New York, 2005.

[3] Abele, E., Weigold, M. and Rothenbücher, S., 'Modleing and Identification of an Industrial Robot for Machining Applications', *Annals of the CIRP*, Vol. 56, 2007, 387-390.
[4] Mohamed, Z. and Tokhi, M. O., 'Command shaping techniques for vibration control of a flexible robot manipulator', *Mechatronics*, 14, 2004, 69-90.
[5] Shabana, A. A., 'Flexible Multibody Dynamics: Review of Past and Recent Developments', *Multibody System Dynamics*, 1, 1997, 189-222.
[6] Online documentation of MD Adams, Version R3, 2009.
[7] S. Umeyama, 'Least-Squares Estimation of Transformation Parameters Between Two point Patterns', IEEE Transaction on pattern analysis and machine intelligence, Vol. 13, No. 4, April 1991, 376-380.

9. BIOGRAPHY

Grzegorz Swiatek is a fourth year undergraduate student in Mechanical Engineering at Écolde de technologie supérieure. He works on this research project through the NSERC Undergraduate Student Research Awards (USRA). His research interests include finite element analysis, dynamic modeling and simulation and 3D CAD of mechanical systems. In the past years, he participated in various computer-aided 3D design competitions including the "WorldSkills" world finals in Japan, during the year of 2007.

Zhaoheng Liu is a professor in Mechanical Engineering at École de technologie supérieure, Université du Québec, Canada. His current research interests include nonlinear dynamics, vehicle dynamics, chatter vibration in robotic manufacturing processes and reliability optimization in mechanical design. He is registered professional engineer in the province of Quebec, members of the American Society of Mechanical Engineers (ASME) and the Canadian Machinery Vibration Association (CMVA).

Bruce Hazel is a researcher in robotics at Hydro-Quebec's research institute (IREQ) in Canada. He is the project leader for the SCOMPI technology. His current research interests include portable robots and manufacturing processes such as welding and grinding. He is registered professional engineer in the province of Quebec.